

Superconducting energy gap in MgB_2 film observed by infrared reflectance.

A. Pimenov¹, A. Loidl¹, and S. I. Krasnosvobodtsev²

¹*Experimentalphysik V, EKM, Universität Augsburg, 86135 Augsburg, Germany*

²*P. N. Lebedev Physics Institute, Russian Academy of Sciences, 117924 Moscow, Russia*

(May 20, 2019)

Far-infrared reflectance of a MgB_2 film has been measured by Fourier-transform spectroscopy for frequencies $10 \text{ cm}^{-1} < \nu < 4000 \text{ cm}^{-1}$ above and below the superconducting transition. The data provide clear experimental evidence for the onset of a superconducting gap at 24 cm^{-1} . From the present results real and imaginary parts of the optical conductivity $\sigma^*(\nu)$ have been calculated taking submillimeter results from earlier measurements into account. At low temperatures $\sigma^*(\nu)$ bears the characteristics of a BCS superconductor.

The discovery of superconductivity in MgB_2 [1] raised the question about the nature of the energy gap in this compound. Among different methods to observe and measure the superconducting energy gap, infrared spectroscopy remains a very promising and powerful method. Indeed, first experiments on grazing infrared reflectivity in MgB_2 [2] showed features of the experimental spectra, which may be attributed to the superconducting gap. The analysis of the data revealed a gap value in the range $2\Delta \simeq 3 - 4 \text{ meV}$. This value is rather small compared to the BCS estimate $2\Delta \approx 12 \text{ meV}$ and has been attributed to the minimum of the gap distribution due to anisotropy.

The infrared-transmission experiments by Jung. *et al.* [3] carried out on MgB_2 thin films revealed a characteristic peak, which could be connected to the energy gap and resembled the predictions of the weak-coupling BCS-theory. These experiments were similar to the classical experiments of Ginsberg and Tinkham on lead, tin and indium [4]. Applying the Kramers-Kronig analysis to the thin-film transmission data of these compounds, a superconducting gap in the real part of the complex conductivity, $\sigma^*(\omega) = \sigma_1 + i\sigma_2$ could be directly observed. In experiments with MgB_2 , Jung. *et al.* [3] restricted the data analysis to the comparison with predictions of the BCS-theory which gave an estimate of the energy gap, $2\Delta_0 \simeq 5.2 \text{ meV}$. Later on, terahertz time-domain spectroscopy has been applied to the transmission of thin MgB_2 films [5]. Due to phase-sensitivity of the time-domain spectroscopy, the complex conductivity of MgB_2 could be extracted from the spectra without application of the Kramers-Kronig analysis. As for classical superconductors, the frequency dependence of σ_1 revealed a characteristic minimum in the frequency dependence, which could be attributed to the superconducting gap, $2\Delta \simeq 5 \text{ meV}$.

While there is already a large scatter of gap values as determined from optical experiments, the gap energies differ even more when values deduced from different experimental setups are compared. Techniques like tunneling spectroscopy [6], photoemission [7,8] or specific heat [9] reveal significantly different values of the energy gap ranging between $2\Delta = 3 - 10 \text{ meV}$. These discrepancies together with the observed deviations from the BCS tem-

perature dependence have been partly explained by imperfections of the sample surface, but alternative explanations based e.g. on multiple gaps [8,10] or anisotropy [11] have also been proposed. For a recent discussion see Ref. [12] and references therein. Different values, observed by various experiments may be partly explained by the preferential sensitivity of particular experiments to different portions of the gap distribution. Probably, optical conductivity methods tend to yield rather the lower limit of the gap distribution. The above-mentioned infrared experiments [2,3,5] revealed the 2Δ values between 3 and 5 meV, i.e. substantially below the BCS estimate.

Previously, we have investigated thin films of MgB_2 using the method of quasioptical spectroscopy in the frequency range $4 \text{ cm}^{-1} < \nu < 30 \text{ cm}^{-1}$ [13]. The highest frequency of this experiment was too low to make distinct conclusions about the spectral gap in $\sigma_1(\omega)$. Therefore, we investigated the same sample at infrared frequencies using the technique of Fourier-Transform spectroscopy. The infrared spectroscopy of thin superconducting films reveals distinct advantages compared to the spectroscopy on bulk samples [14]. The reflectance of bulk superconducting samples rapidly approaches unity both in the normal and in the superconducting state especially at low frequencies. This implies a number of experimental difficulties investigating the changes in reflectance at the superconducting transition. In contrast, the reflectance of thin films can be substantially reduced (compared to unity), which strongly improves the accuracy of the data. In addition, the technique of quasioptical transmission spectroscopy [15] can be applied to the same films at lower frequencies. The transmission technique provides an independent measurement of the complex conductivity at submillimeter frequencies and the reflectance of the sample can be calculated from these data, which strongly expands the low-frequency limit of the available spectrum and substantially improves the quality of the Kramers-Kronig analysis. The combination of these two techniques has been applied previously to thin YBaCuO films [14] and showed the reliability and the advantage of the described procedure compared to conventional far-infrared analyses.

The MgB₂ film has been grown by two-beam laser ablation on a [1102] sapphire substrate. Magnetization measurements have indicated a sharp superconducting transition at 32 K with a width of 1 K. The details of the growth process will be given elsewhere [16]. For further details of the film characterization see Ref. [13]. In the frequency range $10 < \nu < 4000 \text{ cm}^{-1}$ reflectivity measurements were performed using a Bruker IFS-113v Fourier-transform spectrometer. Different sources, beam splitters and optical windows allowed to cover the complete frequency range. A pumped liquid-He bolometer has been employed below 60 cm^{-1} . In addition, the reflectance in the frequency range $4 < \nu < 30 \text{ cm}^{-1}$ has been calculated using the complex conductivity data of the same sample, obtained by the submillimeter transmission [13]. Details of this technique can be found elsewhere [15].

Fig. 1 shows the reflectance of the MgB₂ film for different temperatures. The most striking feature of the data is the change in slope of the reflectance around 24 cm^{-1} . The reflectance below this frequency is close to one at $T = 5 \text{ K}$ and drops rapidly above 24 cm^{-1} . It is important to note that this change in slope is seen in the calculated submillimeter data (symbols) as well. Therefore, we interpret this feature as a direct observation of the spectral gap in MgB₂. For increasing temperatures the "knee" point in reflectance becomes smoothed and slightly shifts to lower frequencies.

The reflectivity of a thin metallic film on a dielectric substrate may be obtained from the Maxwell equations and takes the form [17]:

$$r = \frac{r_{0f} + r_{fs} \exp(4\pi i n_f d / \lambda)}{1 + r_{0f} r_{fs} \exp(4\pi i n_f d / \lambda)}, \quad (1)$$

with $r_{0f} = (1 - n_f)/(1 + n_f)$ and $r_{fs} = (n_f - n_s)/(n_f + n_s)$ being the Fresnel reflection coefficients at the air-film (r_{0f}) and film-substrate (r_{fs}) interface. Here $n_f = (i\sigma^*/\varepsilon_0\omega)^{1/2}$ and n_s are the complex refractive indices of the film and substrate, respectively, λ is the radiation wavelength, d is the film thickness, $\omega = 2\pi\nu$ is the angular frequency, $\sigma^* = \sigma_1 + i\sigma_2$ is the complex conductivity of the film, and ε_0 is the permittivity of free space.

Eq. (1) neglects reflections from the opposite side of the substrate. It has to be noted that especially at low frequencies, interferences within the substrate are observed in the spectra (inset of Fig. 1). In that case the full expression taking into account the finite substrate thickness is more appropriate to calculate the conductivity. However, attempts to carry out the calculation using the exact expression instead of Eq. (1) did not improve the quality of the data. A possible reason for this fact is the insufficient resolution of the interferences. Instead, the interference fringes in the reflectivity spectra have been removed by averaging. The results of the averaging procedure are demonstrated in the inset of Fig. 1 and

do not change the overall frequency dependence of the reflectance.

If the film thickness is smaller than the penetration depth ($|n_f|d \gg \lambda$) and if $|n_f| \gg |n_s|$, Eq. (1) is simplified to :

$$r \approx \frac{1 - \sigma^* d Z_0 - n_s}{1 + \sigma^* d Z_0 + n_s}, \quad (2)$$

where $\sigma^* = -in_f^2 \varepsilon_0 \omega$ is the complex conductivity of the film and $Z_0 = \sqrt{\mu_0/\varepsilon_0} \simeq 377 \Omega$ is the impedance of free space. Eq. (2) is advantageous due to its simplicity and provides a good approximation of the reflectivity at submillimeter frequencies. For higher frequencies Eq. (1) is more appropriate.

The experimentally obtained reflectance $R = |r|^2$ does not provide enough information to calculate the film conductivity because of the unknown phase shift. Therefore, a Kramers-Kronig analysis has to be applied to the reflectance in order to obtain the phase shift. The condition of the applicability of this kind of analysis is the analyticity of $\log|r|$ in the upper half plane [18]. The absence of the poles in $\log|r|$ is ensured by the relation $|r| \leq 1$. The absence of zeros in $|r|$ (i.e. branch points in $\log|r|$) is demonstrated in Fig. 1 and follows from the analysis of the numerator of Eq. (1): the term r_{0f} gives the reflectivity of the metal-vacuum boundary and therefore is close to (-1), the term $r_{fs} \exp(4\pi i n_f d / \lambda)$ is suppressed due to the presence of the exponent.

The general problem in the application of the Kramers-Kronig analysis is the necessity to extend the reflectance spectrum to low and to high frequencies. The high-frequency extrapolation up to 22000 cm^{-1} has been taken from the data of Tu *et al.* [19]. The low-frequency extrapolation, which is the most important for our data analysis, has been obtained from the complex conductivity data of the same film, measured by quasi-optical transmission spectroscopy in the range $4 < \nu < 30 \text{ cm}^{-1}$ [13]. Below 4 cm^{-1} the extrapolations $(1 - r) \propto \omega$ and $r = \text{const}$ have been used in the superconducting and normal conducting state, respectively. These extrapolations follow from Eq. (2) and from the low-frequency limits $\sigma^* \approx i\sigma_2 \propto 1/\omega$ for a superconductor and $\sigma^* \approx \sigma_1$ for a metal. As demonstrated in Fig. 1, the calculated submillimeter data (symbols) overlap and coincide with the measured infrared reflectance (lines) without any arbitrary shifts.

The complex conductivity of the MgB₂ film has been calculated from the reflectance data of Fig. 1 and solving Eq. (1). The complex refractive index of the Al₂O₃ substrate has been obtained in a separate experiment and agrees well with literature data [20]. The reflectivity phase shift of the substrate-film system has been obtained by carrying out the Kramers-Kronig analysis as described above. The results are presented in Fig. 2. The real part of the conductivity (upper panel) is frequency independent in the normal conducting state ($T = 40 \text{ K}$) and

below 100 cm^{-1} . The corresponding imaginary part σ_2 (lower panel) is roughly zero for these frequencies. This picture corresponds well to the low-frequency limit of the Drude-conductivity of a simple metal. On cooling the sample into the superconducting state, σ_1 becomes suppressed between 5 and 100 cm^{-1} and shows a clear minimum, which corresponds to the superconducting gap. The position of the minimum at $T = 5\text{ K}$ corresponds well to the change in slope in reflectance ($\nu \approx 24\text{ cm}^{-1}$, Fig. 1). However, the minimum in σ_1 shifts to *higher* frequencies as the temperature increases. This contradicts the behavior of the "knee" in reflectance and to the expectations for the temperature dependence of the superconducting energy gap. We attribute this unusual observation to extrinsic absorption processes at low frequencies, which mask the intrinsic temperature dependence of the gap.

The suppression of σ_1 at infrared frequencies (upper part of Fig. 2) reflects the reduction of the low-frequency spectral weight. At the same time, σ_2 rapidly increases revealing approximately a $1/\omega$ behavior. From the slope of ω^{-1} the spectral weight of the superconducting condensate can be estimated and turns out to be roughly 20% higher than the reduction of the spectral weight in σ_1 . This possibly indicates that a substantial extrinsic contribution is present in σ_1 in the superconducting state.

Besides the gap feature, an additional excitation is observed in the conductivity spectra for frequencies above 100 cm^{-1} (Fig. 2). This feature is seen as a broad maximum around 230 cm^{-1} , which is only weakly temperature dependent. For frequencies higher than 400 cm^{-1} the conductivity decreases again, which possibly reflects the high-frequency behavior of the Drude-conductivity with a characteristic scattering rate $1/2\pi\tau \approx 400\text{ cm}^{-1}$. At the same frequency a broad maximum becomes apparent in σ_2 (lower part of Fig. 2), a behavior which is expected within the Drude picture. The scattering rate $1/2\pi\tau \approx 400\text{ cm}^{-1}$ roughly corresponds to $1/2\pi\tau \approx 150\text{ cm}^{-1}$, obtained from the low-frequency transmittance of this film [13]. The discrepancies most probably reflect the experimental uncertainties. The origin of the broad maximum in σ_1 on top of the Drude-conductivity is unclear at present. We cannot attribute it to residual effects due to substrate, because the phonon excitations in Al_2O_3 start around 400 cm^{-1} and produce sharp anomalies in the spectra for $400 < \nu < 700\text{ cm}^{-1}$. A possible alternative explanation for the broad maximum could be bound states of localized charge carriers, similar to infrared maxima, observed in Zn-doped $\text{YBa}_2\text{Cu}_3\text{O}_8$ [21].

Finally, Fig. 3 compares the experimental conductivity with the predictions of the weak-coupling BCS-model [22]. The value of the superconducting gap is fixed by the characteristic feature in σ_1 . The scattering rate $1/2\pi\tau = 600\text{ cm}^{-1}$ has been chosen in order to reasonably fit the decrease of σ_1 at high frequencies and the broad maximum in σ_2 around 400 cm^{-1} . This value of

the scattering rate implies the applicability of the dirty limit to MgB_2 . In this limit the changes of the scattering rate have no substantial influence on the complex conductivity below 100 cm^{-1} . We further note that the imaginary part of the conductivity at $T = 5\text{ K}$ is well reproduced by the BCS-model without additional fitting parameters.

For low frequencies and in the superconducting state the σ_1 values are far above the model calculations, a fact that again probably implies an additional absorption due to film imperfections. Above the gap frequency, the theoretical curve shows a slightly higher slope compared to the experiment. Taking into account other data available in literature, this difference may indicate a distribution of gap values.

In conclusion, we presented the far-infrared reflectance of a thin MgB_2 film and combined it to the low-frequency data, obtained by the submillimeter spectroscopy. The broadband reflectance reveals a well-defined change in slope around $\nu \simeq 24\text{ cm}^{-1}$, which we interpret as a direct evidence of the superconducting gap, $2\Delta \simeq 3\text{ meV}$. The complex conductivity at infrared frequencies has been obtained applying the Kramers-Kronig analysis to the reflectance data and solving the equations for the substrate-film system. In the real part of the conductivity a minimum develops in the superconducting state, which corresponds to the gap frequency. In addition, a broad conductivity maximum is observed at $\nu \sim 230\text{ cm}^{-1}$ and is attributed to bound states of localized charge carriers.

We thank F. Mayr, Ch. Hartinger and K. Pucher for help in carrying out the infrared measurements, and S. Six, Ch. Schneider and G. Hammerl for the film characterization. We acknowledge stimulating discussion with A. V. Pronin and H.-A. Krug von Nidda. This work was supported by the BMBF via the contract 13N6917/0 - EKM.

-
- [1] J. Nagamatsu *et al.*, Nature **410**, 63 (2001).
 - [2] B. Gorshunov *et al.*, Eur. Phys. J. B **21**, 159 (2001).
 - [3] J. H. Jung *et al.*, cond-mat/0105180.
 - [4] D. M. Ginsberg and M. Tinkham, Phys. Rev. **118**, 990 (1960).
 - [5] R. A. Kaindl *et al.*, cond-mat/0106342.
 - [6] G. Karapetrov *et al.*, Phys. Rev. Lett. **86**, 4374 (2001); A. Sharoni *et al.*, Phys. Rev. B **63**, 220508 (2001); H. Schmidt *et al.*, Phys. Rev. B **63**, 220504 (2001).
 - [7] T. Takahashi *et al.*, Phys. Rev. Lett. **86**, 4915 (2001).
 - [8] S. Tsuda *et al.*, cond-mat/0104489.
 - [9] F. Bouquet *et al.*, Phys. Rev. Lett. **87**, 047001 (2001); R. K. Kremer *et al.*, cond-mat/0102432; Ch. Wälti *et*

al., cond-mat/0102522; Y. Wang *et al.*, Physica C **355**, 179 (2001).

- [10] E. Bascones and F. Guinea, cond-mat/0103190.
- [11] S. Haas and K. Maki, cond-mat/0104207.
- [12] C. Buzea and T. Yamashita, cond-mat/0108265.
- [13] A. V. Pronin *et al.*, Phys. Rev. Lett. **87**, 097003 (2001).
- [14] A. Pimenov *et al.*, Ferroelectrics, **249**, 165 (2001).
- [15] G. V. Kozlov and A. A. Volkov, in *Millimeter and Submillimeter Wave Spectroscopy of Solids*, edited by G. Grüner (Springer, Berlin, 1998), p. 51.
- [16] S. I. Krasnovobodtsev *et al.*, to be published.
- [17] O. S. Heavens, *Optical properties of thin solid films* (Dover Publ., New York, 1991).
- [18] M. Cardona, in *Optical Properties of Solids*, Edited by S. Nudelman and S. S. Mitra (Plenum Press, New York, 1969), p. 137.
- [19] J. J. Tu *et al.*, cond-mat/0107349.
- [20] A. S. Barker, Jr., Phys. Rev. **132**, 1474 (1963).
- [21] D. N. Basov, B. Dabrowski, and T. Timusk, Phys. Rev. Lett. **81**, 2132 (1998).
- [22] W. Zimmerman *et al.*, Physica C **183**, 99 (1991).

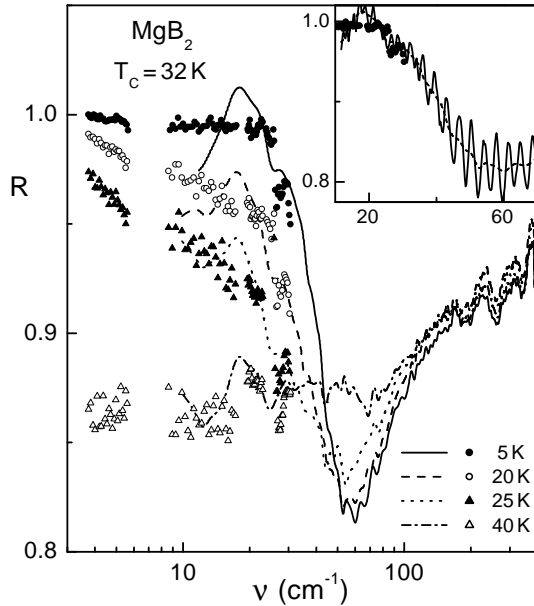


FIG. 1. Far-infrared and submillimeter reflectance of MgB₂ film on an Al₂O₃ substrate. Lines: directly measured reflectance, symbols: data as calculated from the complex conductivity in the submillimeter range [13]. The inset demonstrates the result of the averaging procedure of the interference pattern at $T = 5$ K.

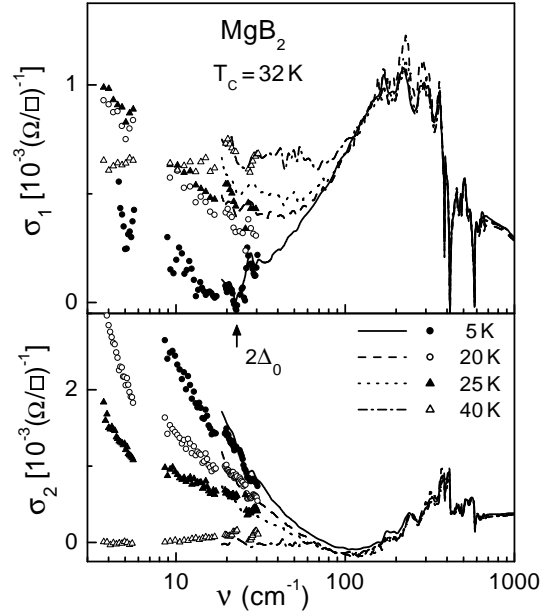


FIG. 2. Complex conductivity of a MgB₂ film at infrared frequencies. Upper panel: real part σ_1 . Lower panel: imaginary part σ_2 . Lines have been obtained via the Kramers-Kronig analysis of the reflectance data. Symbols represent the conductivity, which was directly measured by the transmittance technique [13]. Sharp peak-like structures between 400 and 700 cm⁻¹ is due to residual influence of phonon contribution of the substrate.

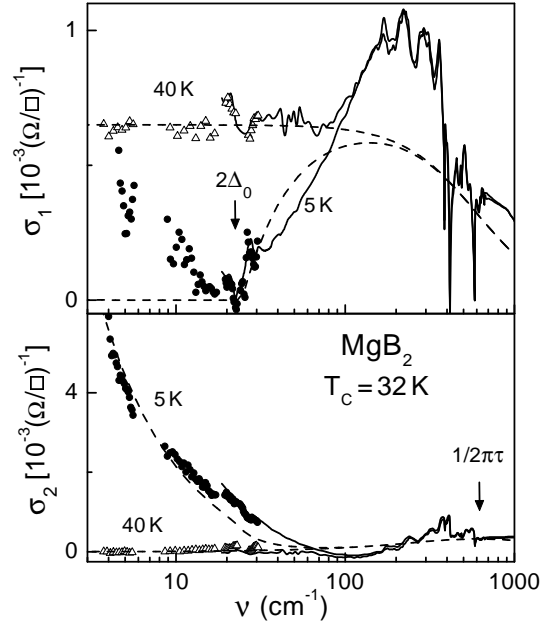


FIG. 3. Comparison between the complex conductivity and the predictions of the weak-coupling BCS-model. Symbols and solid lines represent the experimental data of Fig. 2. Dashed lines: BCS-theory with $2\Delta = 24$ cm⁻¹, $1/2\pi\tau = 600$ cm⁻¹.